WATER RESOURCES RESEARCH, VOL. 29, NO. 4, PAGES 1225–1238, APRIL 1993

Evaluation of a First-Order Water Transfer Term for Variably Saturated Dual-Porosity Flow Models

H. H. GERKE[1] AND M. T. VAN GENUCHTEN

U.S. Salinity Laboratory, U.S. Department of Agriculture, Agricultural Research Service, Riverside, California

Variably saturated water flow in a dual-porosity medium may be described using two separate flow equations which are coupled by means of a sink source term Γ_w to account for the transfer of water between the macropore (or fracture) and soil (or rock) matrix pore systems. In this study we propose a first-order rate expression for Γ_w which assumes that water transfer is proportional to the difference in pressure head between the two pore systems. A general expression for the transfer coefficient α_w was derived using Laplace transforms of the linearized horizontal flow equation. The value of α_w could be related to the size and shape of the matrix blocks (or soil aggregates) and to the hydraulic conductivity K_a of the matrix at the fracture/matrix interface. The transfer term Γ_w was evaluated by comparing simulation results with those obtained with equivalent one- and two-dimensional single-porosity flow models. Accurate results were obtained when K_a was evaluated using a simple arithmetic average of the interface conductivities associated with the fracture and matrix pressure heads. Results improved when an empirical scaling coefficient γ_w was included in α_w. A single value of 0.4 for γ_w was found to be applicable, irrespective of the hydraulic properties or the initial pressure head of the simulated system.

INTRODUCTION

Dual- or double-porosity models, initially introduced to simulate single-phase flow in fissured groundwater reservoirs [e.g., *Barenblatt et al.*, 1960], assume that a porous medium consists of two separate but connected continua. Of these, one continuum is associated with a system or network of fractures, fissures, macropores, or interaggregate pores, while the other continuum involves the porous matrix blocks or soil aggregates. Hence dual-porosity models usually involve two flow equations which are coupled by means of a sink/source term to account for water transfer between the pore systems.

The dual-porosity concept has been popularly used to describe the preferential movement of water and solutes at the macroscopic scale, a phenomenon that is widely believed to occur in most natural (undisturbed) media [e.g., *van Genuchten et al.*, 1990; *Gish and Shirmohammadi*, 1991; *Wang*, 1991]. A large number of double-porosity type models have been proposed to predict water flow in fractured reservoirs [*Barenblatt et al.*, 1960; *Warren and Root*, 1963; *Duguid and Lee*, 1977; *Moench*, 1984] or solute transport during both steady state flow [*Coats and Smith*, 1964; *van Genuchten and Wierenga*, 1976] as well as transient groundwater flow [*Bibby*, 1981]. Recently, attempts have been made to extend the concept to transient water flow and solute transport in variably saturated fractured rock formations and structured soils [*Dykhuizen*, 1987; *Dudley et al.*, 1988; *Peters and Klavetter*, 1988; *Jarvis et al.*, 1991; *Chen and Wagenet*, 1992*a*, *b*; *Gerke and van Genuchten*, 1993].

One of the most critical components of dual-porosity models is the source/sink term describing the exchange of water between the fracture and the matrix pore systems. The interactions between the two pore regions during variably saturated flow are governed by transient, nonlinear local-scale flow processes at and across the fracture/matrix interface. The main challenge is to capture these local-scale, microscopic processes as best as possible into a relatively simple term for use in a macroscopic dual-porosity model.

In this paper we propose a first-order mass transfer term to be used in dual-porosity models for transient water flow in variably saturated structured media. First, we will briefly review previous dual-porosity type models, including alternative ways of formulating the mass transfer term. The review includes a discussion of dual-porosity solute transport models, since they suggest a method for deriving the transfer term proposed in this paper. The transfer term will be evaluated by comparing simulation results with those obtained using equivalent one- and two-dimensional single-porosity unsaturated flow models. For convenience, we will consider only one spatial dimension (vertical flow), ignore the effects of soil water hysteresis, assume that the porous medium is rigid, consider the densities of the fluid and solid phases to be constant, and neglect the effects of temperature, air pressure, and solute concentration on water flow.

BACKGROUND

Dual-Porosity Water Flow Models

A dual-porosity model for variably saturated, one-dimensional vertical water flow in a structured porous medium was proposed by *Gerke and van Genuchten* [1993]. The model involves two Richards' equations as follows:

$$C_f \frac{\partial h_f}{\partial t} = \frac{\partial}{\partial z}\left(K_f \frac{\partial h_f}{\partial z} - K_f\right) - \frac{\Gamma_w}{w_f} \qquad (1a)$$

$$C_m \frac{\partial h_m}{\partial t} = \frac{\partial}{\partial z}\left(K_m \frac{\partial h_m}{\partial z} - K_m\right) + \frac{\Gamma_w}{1 - w_f} \qquad (1b)$$

where (1*a*) and (1*b*) describe the flow of water in the fracture (subscript f) and matrix (subscript m) pore systems, respectively. In these equations, h is the pressure head (L), $C = d\theta/dh$ is the specific water capacity (L^{-1}), θ is the

[1]Now at Cremlingen, Germany.

Paper number 92WR02467.

volumetric water content ($L^3\ L^{-3}$), K is the hydraulic conductivity ($L\ T^{-1}$), w_f denotes the volume of the fracture pore system relative to that of the total soil or rock system, z is depth taken to be positive downward (L), t is time (T), and Γ_w is the mass transfer term for water (T^{-1}). The transfer term is assumed to be proportional to the difference in pressure head between the fracture and matrix pore systems as follows:

$$\Gamma_w = \alpha_w(h_f - h_m) \tag{2}$$

in which α_w is a first-order mass transfer coefficient ($L^{-1}\ T^{-1}$) for water. As will be discussed later, this coefficient is presumed here to be of the form

$$\alpha_w = \frac{\beta}{a^2} K_a \gamma_w \tag{3}$$

where β is a dimensionless geometry coefficient, a is the characteristic half width (L) of the matrix block, K_a is the effective hydraulic conductivity ($L\ T^{-1}$) of the matrix at or near the fracture/matrix interface, and γ_w is a dimensionless scaling factor.

The dual-porosity model given by (1a) and (1b) may be simplified for conditions where transfer of water between the fracture and matrix pore systems is fast relative to the movement of water in the main flow direction. By assuming that the pressure head in the two regions equilibrate instantaneously, the two coupled equations (1a) and (1b) may be combined to yield a single composite flow equation of the form [e.g., *Dykhuizen*, 1987; *Peters and Klavetter*, 1988]

$$[w_f C_f + (1 - w_f)C_m]\frac{\partial h}{\partial t} = \frac{\partial}{\partial z} \cdot \left\{[w_f K_f + (1 - w_f)K_m]\left(\frac{\partial h}{\partial z} - 1\right)\right\} \tag{4}$$

in which the water capacities and hydraulic conductivities of the two pore systems are weighted by w_f and $1 - w_f$, respectively. A major advantage of (4) is that the equation avoids the difficulty of having to specify the water transfer term while still maintaining separate hydraulic properties of the two pore regions. In contrast, all formulations that consider the dynamic interactions between the fracture and matrix pore systems require an explicit description of the water transfer term, Γ_w.

Dual-Porosity Solute Transport Models

Similar to (1a) and (1b), solute transport in a dual-porosity medium may be described by two coupled convection-dispersion equations [e.g., *Gerke and van Genuchten*, 1993] as follows:

$$\frac{\partial}{\partial t}(\theta_f R_f c_f) = \frac{\partial}{\partial z}\left(\theta_f D_f \frac{\partial c_f}{\partial z} - q_f c_f\right) - \theta_f \mu_f c_f - \frac{\Gamma_s}{w_f} \tag{5a}$$

$$\frac{\partial}{\partial t}(\theta_m R_m c_m) = \frac{\partial}{\partial z}\left(\theta_m D_m \frac{\partial c_m}{\partial z} - q_m c_m\right) - \theta_m \mu_m c_m + \frac{\Gamma_s}{1 - w_f} \tag{5b}$$

where c is the solute concentration ($M\ L^{-3}$), D is the dispersion coefficient ($L^2\ T^{-1}$), μ is a first-order decay coefficient (T^{-1}), R is the retardation factor (dimensionless) accounting for equilibrium sorption, and Γ_s is the solute mass transfer term ($M\ L^{-3}\ T^{-1}$). We used for Γ_s the following equation:

$$\Gamma_s = (1 - d)\Gamma_w \phi_f c_f + d\Gamma_w \phi_m c_m + \alpha_s(1 - w_f)\theta_m(c_f - c_m) \tag{6}$$

where

$$d = 0.5\left(1 - \frac{\Gamma_w}{|\Gamma_w|}\right), \qquad \Gamma_w \neq 0 \tag{7a}$$

and

$$\phi_f = w_f \frac{\theta_f}{\theta}; \tag{7b}$$

$$\phi_m = (1 - w_f)\frac{\theta_m}{\theta} \tag{7c}$$

in which d is a dimensionless coefficient defining the direction of flow between the two pore systems, ϕ_f and ϕ_m are dimensionless coefficients relating the solute concentrations of the fracture and matrix pore systems to the unit solute mass of the bulk soil, and α_s is a first-order solute mass transfer coefficient (T^{-1}) characterizing solute exchange by diffusion between the fracture and matrix liquid phases. Notice that the first two terms on the right-hand side of (6) specify the convective contribution to Γ_s, while the third term gives the diffusion contribution. The coefficient α_s is very similar to the mass transfer coefficient α used previously in mobile-immobile type transport models. These models assume steady or transient water flow in the fracture or interaggregate pore system, and the presence of immobile (nonmoving) water inside matrix blocks, soil aggregates, or dead-end pores [*Coats and Smith*, 1964; *Gaudet et al.*, 1977; *Brusseau and Rao*, 1990]. Mobile-immobile transport models are given by the coupled set of equations [e.g., *van Genuchten and Wierenga*, 1976]:

$$\vartheta_f R_f \frac{\partial c_f}{\partial t} + \vartheta_m R_m \frac{\partial c_m}{\partial t} = \vartheta_f D_f \frac{\partial^2 c_f}{\partial z^2} - \vartheta_f v_f \frac{\partial c_f}{\partial z} \tag{8a}$$

$$\vartheta_m R_m \frac{\partial c_m}{\partial t} = \alpha(c_f - c_m) \tag{8b}$$

where, in terms of the notation of this paper, the mobile and immobile regions are indicated with the subscripts f for fracture and m for matrix, respectively, v is the pore water velocity ($L\ T^{-1}$), and ϑ_f and ϑ_m are mobile and immobile water contents per unit bulk soil volume, i.e.,

$$\vartheta_f = w_f \theta_f = \phi_f \theta; \tag{9a}$$

$$\vartheta_m = (1 - w_f)\theta_m = \phi_m \theta \tag{9b}$$

such that $\theta = \vartheta_f + \vartheta_m$. The mass transfer coefficient α in (8b) is related to α_s in (6) by

$$\alpha = \alpha_s \vartheta_m \tag{9c}$$

Although having a conceptual basis, the mass transfer coefficient α in (8*b*) is usually estimated by fitting solutions of (8*a*) and (8*b*) to measured solute concentration distributions. More exact representations of transport in mobile-immobile type dual-porosity media may be obtained with geometry-based models which account for diffusion into aggregates of known size and geometry. Analytical solutions for such geometry-based models are available for a large number of aggregate geometries [e.g., *Pellett*, 1966; *Rasmuson and Neretnieks*, 1980; *van Genuchten*, 1985]. While conceptually attractive, the geometry-based models are probably too complicated mathematically to be useful for most applications. Also, field soils often contain a mixture of aggregates of various sizes and shapes which are not easily described with such models.

Some of the limitations of (8*b*) may be overcome by relating α to the diffusion properties of soil aggregates or soil matrix blocks. This may be done by comparing the first-order formulation with more comprehensive geometry-based descriptions assuming different aggregate geometries. A variety of techniques have been used for this purpose, including Laplace transform comparisons [*Raats*, 1981; *van Genuchten and Dalton*, 1986; *Wilson and Dudley*, 1987; *Sudicky*, 1990], moment analysis [*Parker and Valocchi*, 1986; *Valocchi*, 1990], or the use of algebraic expansions [*Bolt*, 1979]. These studies have shown that the first-order mass transfer coefficient is of the general form

$$\alpha = \beta \vartheta_m D_m^* / a^2 \tag{10}$$

where D_m^* is the effective diffusion coefficient ($L^2\ T^{-1}$) of the immobile pore region (the matrix pore system). Most of the studies mentioned above derived values for β which range from 3 for rectangular slabs to 15 for spherical aggregates, although other studies obtained slightly different values [e.g., *Dykhuizen*, 1987; *Skopp et al.*, 1981].

Mass Transfer Coefficient for Water

The exchange of water between the fracture and matrix pore systems in dual-porosity models may be viewed as a process which, at least mathematically, is quite similar to the diffusional exchange of solutes in mobile-immobile models. For flow in saturated fractured reservoirs, *Barenblatt et al.* [1960] and *Warren and Root* [1963] assumed the water transfer rate to be a linear function of the difference in the averaged macroscopic pressure head between the fracture and matrix pore systems. Employing a mobile-immobile type dual-porosity flow model, *Warren and Root* [1963] proposed a water transfer coefficient which contained, analogous to (3), the hydraulic conductivity of the matrix pore system, a factor reflecting the geometry of the matrix, and a characteristic length of the matrix blocks. They estimated the characteristic length using surface/volume ratios of the matrix blocks. Since *Warren and Root* [1963] assumed quasi-steady state flow in the matrix blocks, their transfer term is valid only for relatively large dimensionless times. To improve the formulation, *Dykhuizen* [1990] applied an integral method using two estimated pressure head profiles, one for early times, i.e., before the (local) pressure front has reached the center of the matrix block, and another for later times after the front has reached the center. The analysis resulted in a second, larger water transfer term for use during the early stages of the transient flow regime.

Stating the analogy of water flow to the diffusion of solutes, *Dykhuizen* [1987] proposed a first-order coefficient for water transfer into spherical aggregates. The coefficient is similar to (3) with $\beta = \pi^2$. *Duguid and Lee* [1977] derived a more complex time-dependent expression for the water transfer term using an analytical solution for flow from tubular fractures into the surrounding matrix. A simpler transfer term for flow in saturated fractured reservoirs was proposed by *Zimmerman and Bodvarsson* [1989*a*]. They also applied an integral method to derive an approximate analytical solution for diffusion of water from fractures into spherical matrix blocks. As in the approach of *Dykhuizen* [1990], a basic assumption in their analysis was that two different linear (local) pressure head profiles in the matrix block will develop, one before and one after the pressure front reaches the center of the sphere. The hydraulic conductivity of the matrix and a shape factor, $1/a^2$, where a is the radius of the sphere, were included in the transfer term.

Zimmerman and Bodvarsson [1989*b*] extended their approach to derive an approximate closed-form solution for one-dimensional adsorption of water into unsaturated matrix blocks. *Zimmerman et al.* [1990] subsequently obtained analytical expressions for the absorption of water in unsaturated matrix blocks of various geometries. They also proposed a scaling term to predict adsorption into irregularly shaped blocks from the solutions for blocks having a known geometry. The scaling term was assumed to be dependent on the material properties and surface/volume relations of the rock matrix blocks. The physically based approaches of *Zimmerman et al.* [1990] are attractive since they lead to closed-form expressions which can be incorporated in dual-porosity models. However, the approximate instantaneous water transfer terms are still functions of a separate (local) time variable. This feature complicates the generality of a numerical dual-porosity model for variably saturated media, especially when the flow regime and boundary conditions are highly transient.

Water transfer into aggregates of variably saturated structured soils has also been described with the help of numerical solutions of the horizontal flow equation [*Hoogmoed and Bouma*, 1980], Green and Ampt approximations [*Davidson*, 1984, 1985; *Beven and Clarke*, 1986], and Philip's one-term infiltration equation involving the sorptivity [*Chen and Wagenet*, 1992*a*]. In addition, several quasi-empirical Darcian-type water transfer terms have been proposed in which flow is assumed to be proportional to the macroscopic pressure head gradient [e.g., *Workman and Skaggs*, 1990; *Othmer et al.*, 1991] or the difference in the degree of saturation [*Jarvis et al.*, 1991], between the macropores and the soil matrix. Instead of using K_a in (3), these formulations contain the hydraulic conductivity of the matrix, $K_m(h_m)$, evaluated at the matrix pressure head, h_m [*Workman and Skaggs*, 1990], or the minimum of $K_f(\theta_f(h_f))$ and $K_m(\theta_m(h_m))$ [*Othmer et al.*, 1991]. This last study also suggested that the characteristic length, a in (3), should be the sum of the half widths of both pore systems, contrary to most other studies (including this one) which assume that a is associated primarily with the radius or half width of the matrix structures.

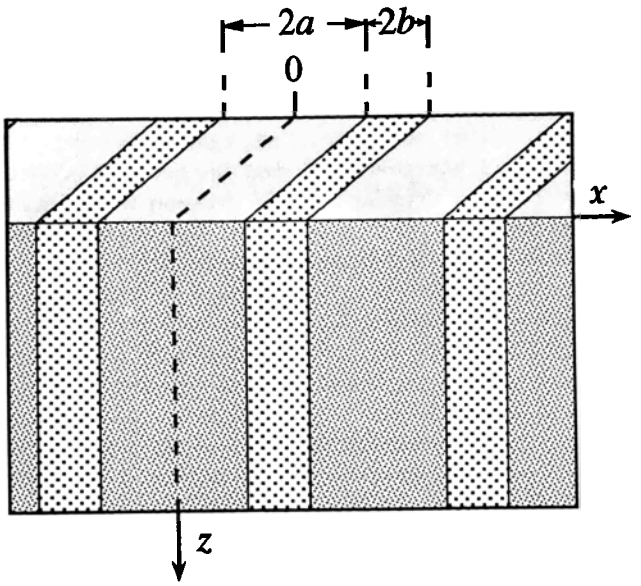

Fig. 1. Schematic illustration of rectangular porous matrix blocks of width $2a$. The blocks, arranged as parallel slabs, are separated by a fracture pore system of width $2b$.

METHODOLOGY

Derivation of the Water Transfer Coefficient

We first derive an equation for the water transfer coefficient, α_w, in (2) following an approach similar to that used by *van Genuchten and Dalton* [1986] for deriving the solute mass transfer coefficient. Let us consider a one-dimensional vertical dual-porosity medium in which the matrix blocks form parallel rectangular slabs (Figure 1) with a half width a between the center of the slab at $x = 0$, and the fracture boundary at $x = a$. For the purpose of deriving an expression for α_w, we momentarily consider only horizontal flow and ignore any vertical water movement in both pore systems. We further assume that the matrix pore system is much larger than the fracture system, and hence that water transfer into the matrix is governed primarily by the dynamics of water flow inside the matrix blocks. For parallel rectangular slabs as shown in Figure 1, horizontal flow at any point in the profile is described with

$$C_a(x; h_a)\frac{\partial h_a(x, t)}{\partial t} = \frac{\partial}{\partial x}\left[K_a(x; h_a)\frac{\partial h_a(x, t)}{\partial x}\right] \qquad (11)$$

$$0 \le x \le a$$

where the subscript a is used to denote evaluation at the local (soil matrix or soil aggregate) level and x is the horizontal coordinate (L). We will compare solutions of (11) with those based on the approximate first-order rate expression

$$\Gamma_w \approx (1 - w_f)C_m(h_m)\frac{dh_m(t)}{dt} = \alpha_w[h_f(t) - h_m(t)] \qquad (12)$$

describing water transfer at the macroscopic level. Equation (12) is consistent with (1*b*) and (2) if vertical flow is neglected.

First, we linearize the coefficients K_a and C_a in (11) to obtain

$$(1 - w_f)C_m(h_m)\frac{\partial h_a(x, t)}{\partial t} - K_a(\hat{h})\frac{\partial^2 h_a(x, t)}{\partial x^2} = 0 \qquad (13)$$

where $K_a(\hat{h})$ represents the effective hydraulic conductivity ($L\,T^{-1}$) of the soil matrix near the fracture/matrix interface, evaluated at some average pressure head $\hat{h}$, to be discussed later. Notice that the coefficients $(1 - w_f)C_m$ and K_a in (13) are now related to the bulk volume of the porous medium. The following initial and boundary conditions are applied:

$$h_a(x, 0) = h_{m,i} \qquad 0 \le x \le a \qquad (14)$$

$$\partial h_a(0, t)/\partial x = 0 \qquad t > 0 \qquad (15a)$$

$$h_a(a, t) = h_f \qquad t > 0 \qquad (15b)$$

where $h_{m,i}$ is the initial pressure head of the soil or rock matrix and h_f is the imposed pressure head at the fracture boundary ($x = a$). Both $h_{m,i}$ and h_f are considered here to be constant in time. The average macroscopic pressure head $h_m(t)$ of the matrix is related to the local pressure head $h_a(x, t)$ by

$$h_m(t) = \frac{1}{a}\int_0^a h_a(x, t)\,dx \qquad (16)$$

Taking the Laplace transform of (13), using (14) and (15*a*) and (15*b*), solving for the Laplace transform, $\bar{h}_a$, and integrating over the matrix block using (16), gives the following solution for h_m in the Laplace domain [e.g., *Carslaw and Jaeger*, 1950, p. 251]:

$$\bar{h}_m(s) = \left(\frac{h_f - h_{m,i}}{s}\right)\frac{\tanh(\xi)}{\xi} + \frac{h_{m,i}}{s} \qquad (17)$$

where s is the Laplace variable, $\bar{h}_m$ is the transformed pressure head of the soil/rock matrix, and $\xi = a[(1 - w_f)C_m s/K_a]^{0.5}$. Substituting the first two terms of the expansion $\tanh(\xi) = \xi - \xi^3/3 + \cdots$, which holds for small ξ and hence large times, into (17) and rearranging leads to

$$\bar{h}_m(s) = \frac{h_f}{s}\left[1 - \frac{a^2(1 - w_f)C_m s}{3K_a}\right] + \frac{h_{m,i}}{s}\left[\frac{a^2(1 - w_f)C_m s}{3K_a}\right] \qquad (18)$$

which is an approximate solution for $\bar{h}_m(s)$ in terms of parameters appearing in the local flow equation (11).

We can similarly take the Laplace transform of (12), use again an initial pressure head $h_{m,i}$, assume h_f to be constant in time, and rearrange, to obtain

$$\bar{h}_m(s) = \frac{h_f}{s}\left(\frac{1}{1 + \zeta}\right) + \frac{h_{m,i}}{s}\left(\frac{1}{1 + \zeta^{-1}}\right) \qquad (19)$$

where $\zeta = s(1 - w_f)C_m/\alpha_w$. Using the approximations $1/(1 + \zeta) \approx 1 - \zeta$ and $1/(1 + \zeta^{-1}) \approx \zeta$ for relatively small ζ gives

$$\bar{h}_m(s) = \frac{h_f}{s}\left[1 - \frac{(1 - w_f)C_m s}{\alpha_w}\right] + \frac{h_{m,i}}{s}\left[\frac{(1 - w_f)C_m s}{\alpha_w}\right] \qquad (20)$$

which is the solution for $\bar{h}_m(s)$ derived from (12). Equating (18) with (20) yields the following expression for α_w assuming rectangular slabs:

$$\alpha_w = \frac{3}{a^2} K_a \tag{21}$$

This equation has a form analogous to (10) for the solute mass transfer coefficient. We note that the same result can be obtained also for a time-dependent boundary condition $h_f(t)$ in (15b). The only difference is that h_f/s in (17) through (20) is replaced by its Laplace transform $\bar{h}_f$.

Transfer coefficients for other geometries, such as spherical, solid or hollow cylindrical structures, may be derived in the same manner. The equations are the same as those for solute mass transfer [*van Genuchten*, 1985; *van Genuchten and Dalton*, 1986; *Sudicky*, 1990; *Valocchi*, 1990], provided that the effective diffusion coefficient D_m^* is replaced by the effective hydraulic conductivity K_a.

Macroscopic Scaling of the Water Transfer Coefficient

The analytically derived term (21) was evaluated by directly comparing results obtained with a numerical solution of (11) with those calculated using (12) and (21). Horizontal infiltration of water in the matrix blocks was simulated using a modified version of the HYDRUS code [*Kool and van Genuchten*, 1991] in which the gravity term was eliminated. HYDRUS solves (11) using a fully implicit, mass-lumped Galerkin finite element scheme assuming linear basis functions. To minimize numerical errors, extremely small space and time steps ($\Delta t \approx 10^{-7} - 10^{-6}$ days; $\Delta x = 5 \times 10^{-5}$ m) were used in the calculations.

The nonlinear first-order rate equation (12), subject to the initial condition $h_m(t = 0) = h_{m,i}$, was solved by rewriting the equation in the following discretized form:

$$\Gamma_w \approx (1 - w_f) C_m \frac{\Delta h_m}{\Delta t} = \alpha_w [h_f - h_m(t)] \tag{22}$$

which in turn was approximated by the time-centered scheme

$$h_m(t + \Delta t) = h_m(t) + \frac{\alpha_w^{t + 1/2\Delta t} \Delta t}{(1 - w_f) C_m} [h_f - h_m(t + 1/2\Delta t)] \tag{23}$$

where the superscript $t + 1/2\Delta t$ on α_w indicates evaluation at the half time level. Because of nonlinearities resulting from $C_m(\theta_m(h_m))$ and $K_a(\hat{h})$, (23) was solved iteratively at each time step using a procedure analogous to that employed in HYDRUS for solving the Richards' equation [*Kool and van Genuchten*, 1991].

TABLE 1. Assumed Hydraulic Parameters for the Horizontal and Two-Dimensional Flow Simulations

	θ_r	θ_s	α, cm^{-1}	n	K_s, cm/d
Texture					
Coarse	0.05	0.40	0.0100	2.50	1.0
Medium	0.10	0.45	0.0020	1.60	1.0
Fine	0.15	0.50	0.0005	1.25	1.0
Pore System					
Matrix	0.10526	0.5	0.005	1.5	1.0526
Fracture	0.0	0.5	0.1	2.0	2000.0

In the analysis below, mass transfer, horizontal infiltration, and water flow in the matrix blocks, were simulated using hydraulic properties (Table 1) typical of relatively fine, medium-, and coarse-textured soils. The hydraulic functions were described with the equations [*van Genuchten*, 1980]

$$\theta = \theta_r + \frac{\theta_s - \theta_r}{[1 + |\alpha h|^n]^m} \tag{24}$$

$$K(S_e) = K_s S_e^{0.5} [1 - (1 - S_e^{1/m})^m]^2 \tag{25}$$

$$m = 1 - 1/n; \quad n > 1$$

where θ_r and θ_s are the residual and saturated water contents, respectively; h is the pressure head, K_s is the hydraulic conductivity at saturation, $S_e = (\theta - \theta_r)/(\theta_s - \theta_r)$ is effective saturation, and α and n are empirical parameters. To simplify the analysis, the saturated hydraulic conductivity, K_s, of the matrix was set to unity. All simulations assumed that the fracture system, which forms the boundary of the soil or rock matrix block, was saturated ($h_f = 0$ cm).

Figure 2a compares the cumulative horizontal infiltration curve $I(T)$, as calculated with (11) and shown by the dashed reference curve, with cumulative water transfer rates, $T(t) = \int_0^t \Gamma_w \, dt$, obtained using various solutions of approximation (12), for the medium-textured soil. The calculations are for an initial pressure head $h_{m,i}$ of -1000 cm, assuming rectangular matrix blocks ($\beta = 3$) and a soil matrix half width a of 1 cm. The results in Figure 2 were obtained using the following five alternative methods for evaluating the effective hydraulic conductivity $K_a(\hat{h})$ in (21):

Matrix (Mat) $$K_a = K_a(h_m) \tag{26a}$$

Fracture (Fra) $$K_a = K_a(h_f) \tag{26b}$$

Arithmetic (Ari) $$K_a = 0.5[K_a(h_f) + K_a(h_m)] \tag{26c}$$

Geometric (Geo) $$K_a = [K_a(h_f) K_a(h_m)]^{0.5} \tag{26d}$$

Integral (Int) $$K_a = \frac{1}{(h_f - h_m)} \int_{h_m}^{h_f} K_a(h) \, dh \tag{26e}$$

Case Fra may be viewed as an upstream weighting method using $h = \max(h_f, h_m)$, while Int requires numerical integration for certain hydraulic conductivity functions.

In absolute terms (Figure 2a), the first-order results based on (12) show significant deviations from the reference curve. The closest fit was obtained with Int. The Fra and Ari methods overpredicted, and Mat severely underestimated, cumulative infiltration, while Geo gave results which were somewhat intermediate. Notice that Int matched the reference curves at approximately 50% of the total infiltration. This result was also obtained for the coarse- and fine-textured soils and is consistent with a study by *Warrick* [1991], who showed that the integral method produces excellent estimates of the average hydraulic conductivity when simulating horizontal infiltration using a fully discretized system. The large differences among the calculated curves in Figure 2a demonstrate the importance of properly evaluating the effective hydraulic conductivity K_a in (21).

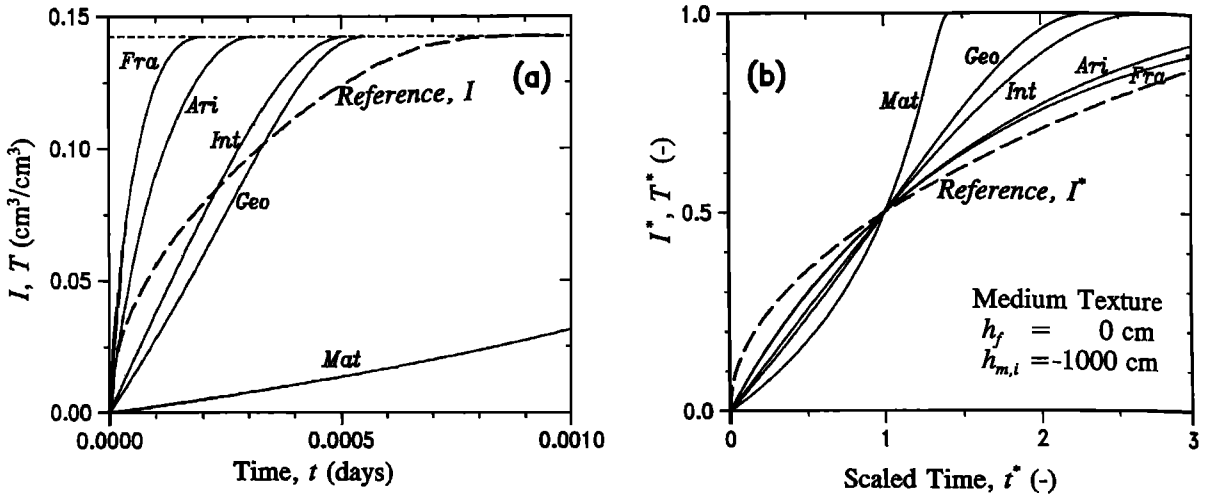

Fig. 2. Cumulative horizontal infiltration I (dashed reference curves) and cumulative water transfer T (solid curves) versus time t for a medium-textured soil in terms of (a) absolute and (b) scaled values, as calculated with different approximations of the hydraulic conductivity K_a at the fracture/matrix interface ($\beta = 3$; $a = 1$ cm).

Qualitatively very similar differences among the curves were observed for the other two soils in Table 1.

In order to reduce the observed differences between the approximate cumulative water transfer curves and the reference results, we used a scaling method analogous to the method used by *van Genuchten* [1985] for solute diffusion in soil matrix blocks. Scaling was accomplished by defining a relative cumulative horizontal infiltration rate as follows:

$$I^* = I(t)/I(\infty) \equiv T(t)/T(\infty) \tag{27}$$

where $I(\infty)$ and $T(\infty)$ are the maximum possible amounts of horizontal infiltration and water transfer into the finite matrix blocks, respectively. Similarly, a relative time can be defined as

$$t^* = t/t_{0.5}; \qquad t_{0.5} = t(I^*)|_{I^*=0.5} \tag{28}$$

where $t^* = 1$ occurs at time $t = t_{0.5}$ when half of the maximum amount of water has infiltrated into the matrix. As shown in Figure 2b, the effect of scaling is to force the approximate first-order solutions to be identical to the complete solution at the point $I^* = 0.5$, $t = t_{0.5}$. The scaling method was implemented by simply introducing an empirical scaling factor γ_w into (21) to yield (3). Formally, γ_w is defined by

$$\gamma_w = t_{0.5}^T/t_{0.5}^I \tag{29}$$

where the superscripts T and I refer to the first-order approximate and complete numerical solutions, respectively.

Whereas the matrix flux potential (Int) gave the best results in absolute terms (Figures 2a), the upstream weighted (Fra) and arithmetic-averaged (Ari) methods after scaling provided the best match with the reference simulation over the entire range of the curves (Figure 2b). Still, the results reflect a tendency by the first-order solutions to initially underestimate and later, for $t^* > 1$, to overestimate cumulative infiltration. Deviations from the reference curves were smallest in both sections of the curves when Fra or Ari were used to evaluate K_a. As shown by the data in Table 2, the scaling coefficients γ_w for these two methods were also found to be less dependent on the soil hydraulic properties as compared to other methods.

Of the various methods, notably Fra, Ari, and Int, we judged the arithmetic averaging (Ari) method, combined with the use of a scaling coefficient, to be the most practical way of evaluating K_a in the proposed dual-porosity models. As opposed to upstream weighing (Fra), Ari considers the pressure heads of both pore systems. This feature may be an advantage when simulating water transfer in both directions in response to varying initial and boundary conditions. Also, the matrix flux potential formulation (Int) requires additional computations for numerical integration of (26e) when using conductivity models such as (25). Hence, in the analysis below we will evaluate K_a exclusively using the arithmetic averaging method given by (26c).

The possibility of achieving better results using more nonlinear expressions for Γ_w was studied next. For this purpose we introduced an exponent, p, into (22) to obtain

$$\Gamma_w = \alpha_w[h_f - h_m(t)]^p \tag{30}$$

Figure 3 presents calculated cumulative infiltration and water transfer rates for the medium-textured soil type, again in terms of the original variable (Figure 3a) and the scaled variable (Figure 3b). The results in Figure 3a show a considerable effect of p on the transfer rates. However, the influence of p on the scaled curves in Figure 3b is relatively small. An increase in p resulted in a slightly better fit at early times ($t^* < 1$) but gave worse results at later times ($t^* > 2$). Similar effects were also found for the coarse- and fine-textured soils (results not shown here). We also noticed that for all three soil types, larger values of p required increas-

TABLE 2. Horizontal Infiltration Data and Scaling Coefficients γ_w for Different Methods of Evaluating K_a ($h_{m,i} = -1000$ cm)

Texture	$I(\infty)$, m^3/m^3	$t_{0.5}^I$, 10^{-4} days	γ_w Mat	Fra	Ari	Geo	Int
Coarse	0.3390	8.46	3162.	0.29	0.58	11.11	1.29
Medium	0.1425	1.63	10.39	0.22	0.43	1.45	1.17
Fine	0.0237	0.27	3.02	0.20	0.37	0.77	1.18

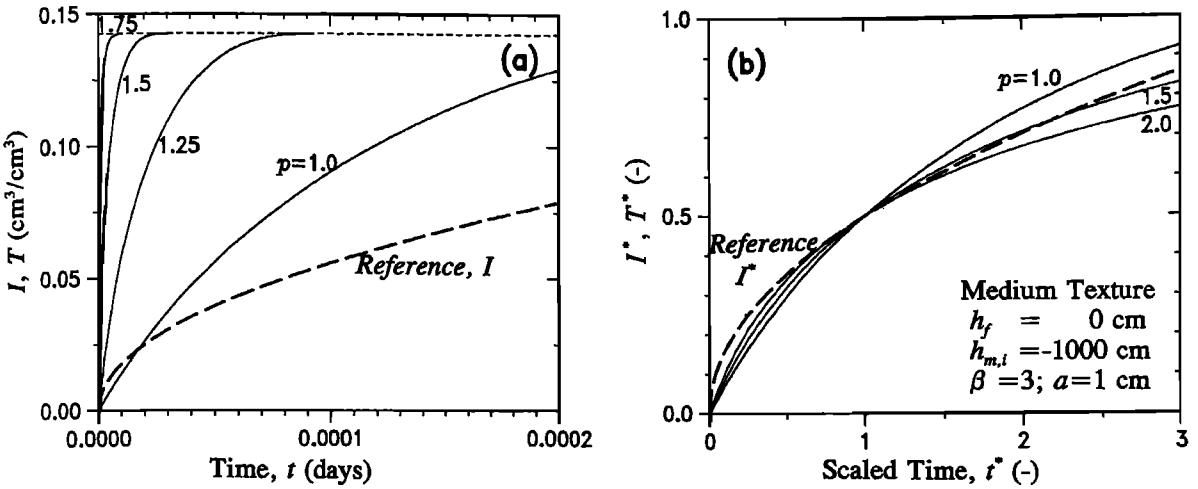

Fig. 3. Cumulative horizontal infiltration I (dashed reference curves) and cumulative water transfer T (solid curves) versus time t for a medium-textured soil in terms of (a) absolute and (b) scaled values, as calculated with different values of p using an arithmetic-averaged K_a (Ari).

ingly smaller values for the scaling coefficient, γ_w, to match the reference curves at $t^* = 1$ (see also Table 3).

The results above were obtained with an initial pressure head $h_{m,i}$ of -1000 cm in the matrix blocks. We investigated the effect of $h_{m,i}$ on the calculations by varying the initial conditions from -30 to $-15{,}000$ cm. Figure 4 gives one set of scaled curves for the medium-textured soil using $p = 1.0$, $a = 1$ cm, and $\beta = 3$ (the other soils again gave very similar results). The corresponding scaling coefficients are listed in Table 3. Notice that the shapes of the scaled water transfer rate curves (Figure 4a) are reasonably similar to those of the reference results (Figure 4b), especially for the lower values of $h_{m,i}$. The scaled cumulative horizontal infiltration curves (Figure 4b) match each other nearly exactly, irrespective of the initial condition, until approximately $t^* = 2.0$. For larger times ($t^* \approx >2$), the scaled infiltration increases slightly when $h_{m,i}$ decreases.

From Figures 3 and 4, as well as from many other calculations not further shown here, we found that in terms of the scaled variables, the first-order term with $p = 1.0$ always underestimated infiltration as calculated with the complete numerical solution at relatively early times (i.e., for $t^* < 0.5$). The two methods produced similar curves when $0.5 < t^* < 2.0$, while the first-order solution overpredicted infiltration by up to 10–20% when $t^* > 2.0$. Also, the scaling coefficient γ_w was found to depend relatively more on the initial pressure head gradient between the two pore systems than on soil type. Table 3 shows that the

TABLE 3. Horizontal Infiltration Data and Scaling Coefficients γ_w for Different Initial Conditions $h_{m,i}$ and Values of p

$h_{m,i}$, cm	$I(\infty)$, m^3/m^3	$t^I_{0.5}$, 10^{-4} days	γ_w				
			$p = 1.0$	$p = 1.25$	$p = 1.50$	$p = 1.75$	$p = 2.00$
			Coarse				
−30	0.0100	0.56	1.29	0.571	0.252	0.111	0.0491
−100	0.1191	3.33	1.23	0.410	0.136	0.0453	0.0150
−330	0.2933	7.49	0.73	0.202	0.056	0.0157	0.0044
−1,000	0.3390	8.46	0.58	0.154	0.041	0.0109	0.00297
−3,000	0.3479	8.87	0.54	NC	NC	NC	NC
			Medium				
−30	0.0015	0.10	1.13	0.512	0.231	0.104	0.0467
−100	0.0095	0.26	1.05	0.352	0.117	0.0391	0.0131
−330	0.0504	0.72	0.79	0.198	0.049	0.0125	0.00313
−1,000	0.1425	1.63	0.43	0.085	0.017	0.0034	0.00067
−3,000	0.2330	2.47	0.23	0.039	0.007	0.0013	0.00019
−15,000	0.3046	3.15	0.12	NC	NC	NC	NC
			Fine				
−30	0.0004	0.04	1.32	0.403	0.184	0.084	0.039
−100	0.0016	0.07	0.76	0.255	0.086	0.029	0.0099
−330	0.0069	0.14	0.58	0.145	0.037	0.009	0.0024
−1,000	0.0237	0.27	0.37	0.070	0.014	0.0026	0.00051
−3,000	0.0622	0.53	0.19	0.029	0.004	0.0007	0.00009
−15,000	0.1418	1.08	0.06	NC	NC	NC	NC

NC indicates no convergence in the numerical solution of the flow equation.

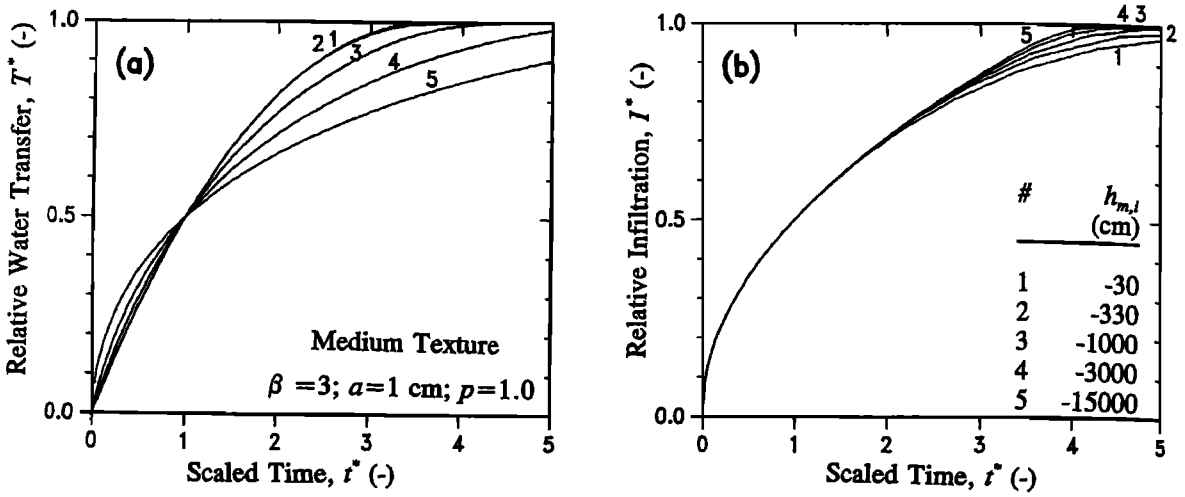

Fig. 4. (*a*) Relative cumulative water transfer T^* and (*b*) relative cumulative horizontal infiltration I^* versus scaled time t^* for a medium-textured soil as calculated with different initial pressure heads $h_{m,i}$ using an arithmetic averaged K_a (Ari) and an imposed fracture boundary pressure head h_f of 0 cm.

dependency of γ_w on $h_{m,i}$ increased considerably with increasing p values. This dependency of γ_w on the initial condition, especially for larger p values, could in principle be taken into account by making γ_w in (3) or (30) a function of $h_{m,i}$. This approach is not followed here since (1) preliminary results indicated only minor improvements in the dual-porosity simulations, even for relatively large differences in γ_w-values such as those shown in Table 3, (2) the functional form $\gamma_w(h_{m,i})$ would depend also on soil type and the value of p, and (3) additional parameters would be introduced, thus limiting the general character of our formulation. Instead, we prefer to use a constant γ_w value, independent of the initial condition and the type of soil involved. Based on the data in Table 3, and further validated below by a series of two-dimensional simulations, we selected a value of 0.4 for γ_w and assumed p = 1.0.

Comparisons With Two-Dimensional Calculations

The first-order transfer term (2) using coefficient (3) with β = 3 will now be evaluated in terms of the complete one-dimensional numerical dual-porosity formulation given by (1) through (3). The applicability of the proposed coupling term with different values of the scaling coefficient, γ_w, will be tested by comparing simulation results with those generated using an equivalent two-dimensional variably saturated flow model. Equations (1), (2), and (3), subject to appropriate initial and boundary conditions, were solved using the numerical model of *Gerke and van Genuchten* [1993]. This model solves the coupled system of equations using a mass-lumped Galerkin finite element scheme. For the two-dimensional reference simulations we used the SWMII model of *Vogel* [1987]. SWMII solves the two-dimensional flow equation using the Galerkin method assuming triangular finite elements. The rectangular slab-type geometry of the porous matrix was imitated by dividing the medium into two vertical layers representing the matrix and fracture pore systems, respectively. Only the half widths of the fracture b and the matrix a pore systems were considered because of symmetry. As shown in Figure 5, the finite element grid was compressed at the boundary between the two regions to enable relatively accurate simulations of the flow process at and across the fracture/matrix interface. Results were obtained using a total of 6800 elements and a self-adapting time-stepping algorithm with an initial time step Δt of usually 10^{-6} days. Most two-dimensional model calculations discussed below used about 70 hours on a IBM compatible AT 486 type, 33-Mhz personal computer to simulate an infiltration period of 0.08 days. By comparison, the dual-porosity model required 20–40 min to run the different examples.

We considered two scenarios. In the first scenario we neglected vertical flow in the matrix pore system, thus creating a mobile-immobile type system in which water transfer and lateral flow across the fracture/matrix interface can be precisely compared. This case expands upon the previous horizontal infiltration example by allowing the boundary pressure head in the fracture pore system to

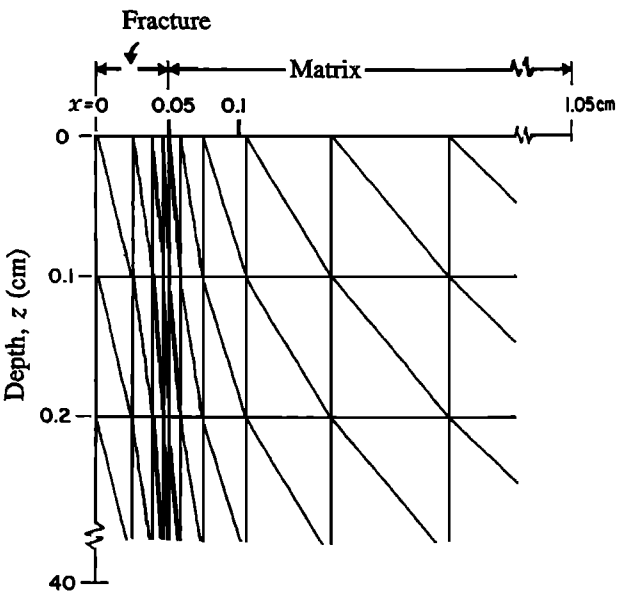

Fig. 5. Finite element grid used in the two-dimensional reference simulations.

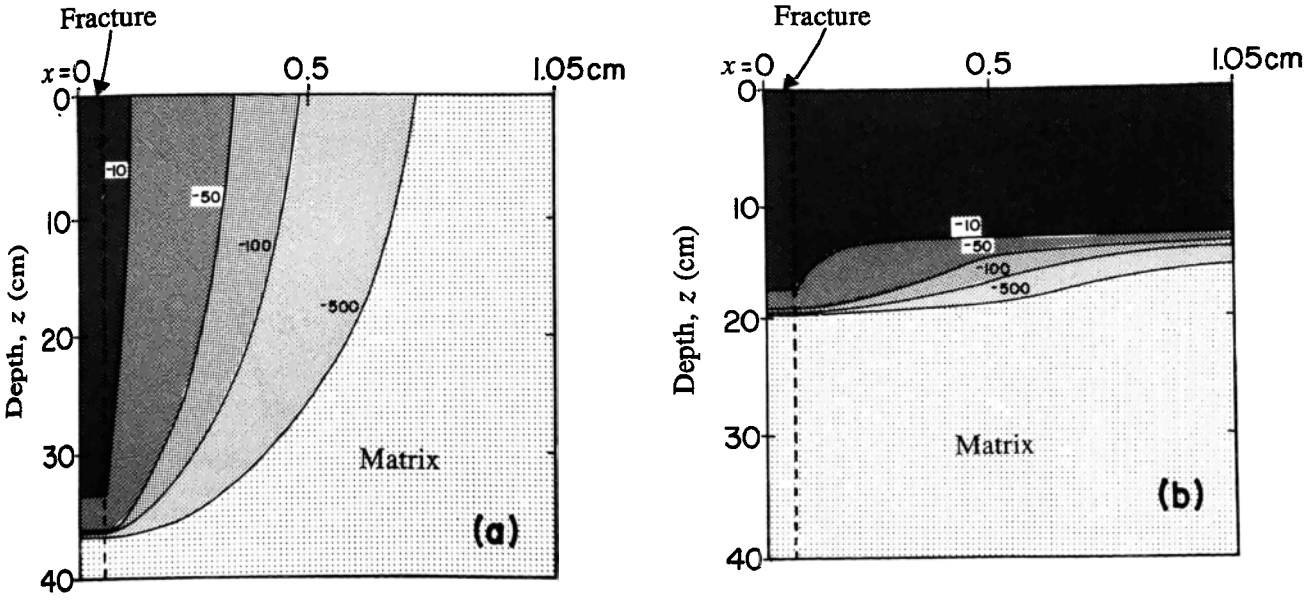

Fig. 6. Pressure head distribution $h_a(x, z, t)$ at $t = 0.08$ days obtained with the two-dimensional model, for (a) relatively low ($K_{s,a} = 0.01$ cm/d) and (b) relatively high ($K_{s,a} = 0.1$ cm/d) water transfer rates.

become time-dependent. The second scenario considers the complete two-dimensional description involving horizontal and vertical flow in both pore systems. The matrix hydraulic conductivity in the two-dimensional model was simulated by employing anisotropy factors of $K_{xx} = K_{s,a}/[(1 - w_f)K_{s,m}]$ for the horizontal direction, and factors of $K_{zz} = 0.0$ (first scenario) and $K_{zz} = K_{xx}$ (second scenario) for the vertical direction. ($K_{s,m}$ is the saturated hydraulic conductivity of the matrix pore system.)

The calculations below pertain to a dual-porosity type structured medium involving a medium- to fine-textured matrix and a coarse-textured fracture pore system with hydraulic parameters as listed in Table 1. We again consider a matrix block size of 2 cm ($a = 1$ cm), and assume that the fracture system makes up 5% of the bulk soil ($w_f = 0.05$), which gives a fracture half width b of 0.05263 cm. We further assume that the soil surface of the matrix is sealed and that water infiltrates at a (local) rate $q_{f,0}$ of 1000 cm/d exclusively into the fracture pore system of a 40-cm-deep dual-porosity medium having an initially uniform pressure head of $h_{f,i} = h_{m,i} = -1000$ cm. Hence the infiltration rate for the bulk soil as a whole q_0 equals 50 cm/d.

Figure 6 shows calculated two-dimensional pressure head distributions at $t = 0.08$ days for scenario one assuming situations with relatively low ($K_{s,a} = 0.01$ cm/d; see Figure 6a) and high ($K_{s,a} = 0.1$ cm/d; see Figure 6b) water transfer rates between the fracture and matrix pore regions. Notice that the horizontal axis is enlarged 40 times. The example in Figure 6a represents a case of significant preferential flow where an infiltration front moves through the 40-cm soil profile in nearly 2 hours. Figure 6a shows considerable lateral pressure head nonequilibrium between the fracture and the matrix, as well as significant variations within the matrix pore region itself. The example in Figure 6b, on the other hand, illustrates the case where equilibrium between the two regions is essentially reached within 10 cm from the moisture front. We will use the calculations in Figure 6 as our reference results.

To effectively compare simulation results of the one-dimensional dual-porosity and two-dimensional single-porosity models, local water contents in the two-dimensional model were averaged over each horizontal line of nodes according to

$$\hat{\theta}_f = \frac{1}{W_f}\sum_{i=1}^{N_f} \theta_{f,i} w_i \qquad \hat{\theta}_m = \frac{1}{W_m}\sum_{i=1}^{N_m} \theta_{m,i} w_i \quad (31)$$

where $\hat{\theta}_f(z)$ and $\hat{\theta}_m(z)$ are the depth-dependent average volumetric water contents of the fracture and matrix pore regions, respectively; N is the number of nodes; θ_i is the nodal volumetric water content in the x direction; W is the width of the fracture or matrix pore system; and w is the width associated with each node i. The average water contents were subsequently used to calculate the rates of horizontal infiltration into the matrix pore region as a function of depth, equivalent to the water transfer rate Γ_w of the dual-porosity model, and to compute average pressure head values in the fracture and matrix pore systems by using the inverse of the retention function.

Figures 7 and 8 compare simulation results obtained with the two-dimensional single-porosity and one-dimensional dual-porosity models using different values of γ_w and p for the first scenario (no vertical flow in the matrix) and the lower water transfer rate ($K_{s,a} = 0.01$ cm/d) at $t = 0.08$ days (1:55 hours). The location of the moisture front in the fracture pore system was found to be a very sensitive indicator of the relative accuracy of the one-dimensional dual-porosity model, including the adopted transfer term. The sensitivity was particularly high in our example because of the relatively small water capacity of the fracture pore system. A small capacity permits small differences in the water transfer rates to produce relatively large variations in the vertical water flow rate.

Figure 7 indicates that the dual-porosity model yields unacceptable results when the first-order term is used without scaling ($p = 1.0$, $\gamma_w = 1.0$). The infiltration front was

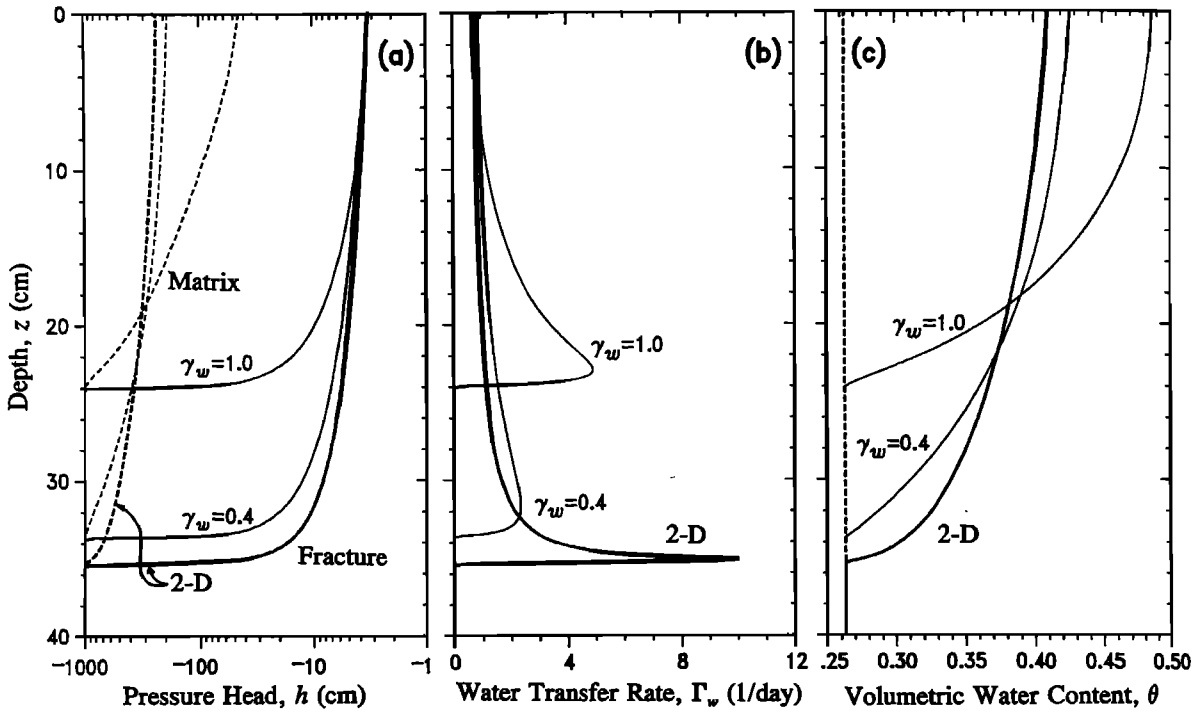

Fig. 7. (*a*) Pressure head h, (*b*) water transfer rate Γ_w, and (*c*) total volumetric water content θ versus depth z at t = 0.08 days as calculated with the one-dimensional dual-porosity (Dual) and two-dimensional (2-D) models. Results are for different scaling coefficients γ_w (first scenario, with p = 1.0, β = 3, a = 1 cm, and $K_{s,a}$ = 0.01 cm/d). The total volumetric water content is defined as $\theta = w_f\theta_f + (1 - w_f)\theta_m$.

more than 11 cm behind the two-dimensional reference simulation. Also, the water transfer rates (Figure 7*b*) and the volumetric water contents (Figure 7*c*) were distributed quite differently over the profile as compared to the two-dimensional reference results. Using p = 1.0 and a single scaling coefficient of 0.4 for γ_w led to a much better agreement with the two-dimensional results for both the pressure head (Figure 7*a*) and the water content (Figure 7*c*);

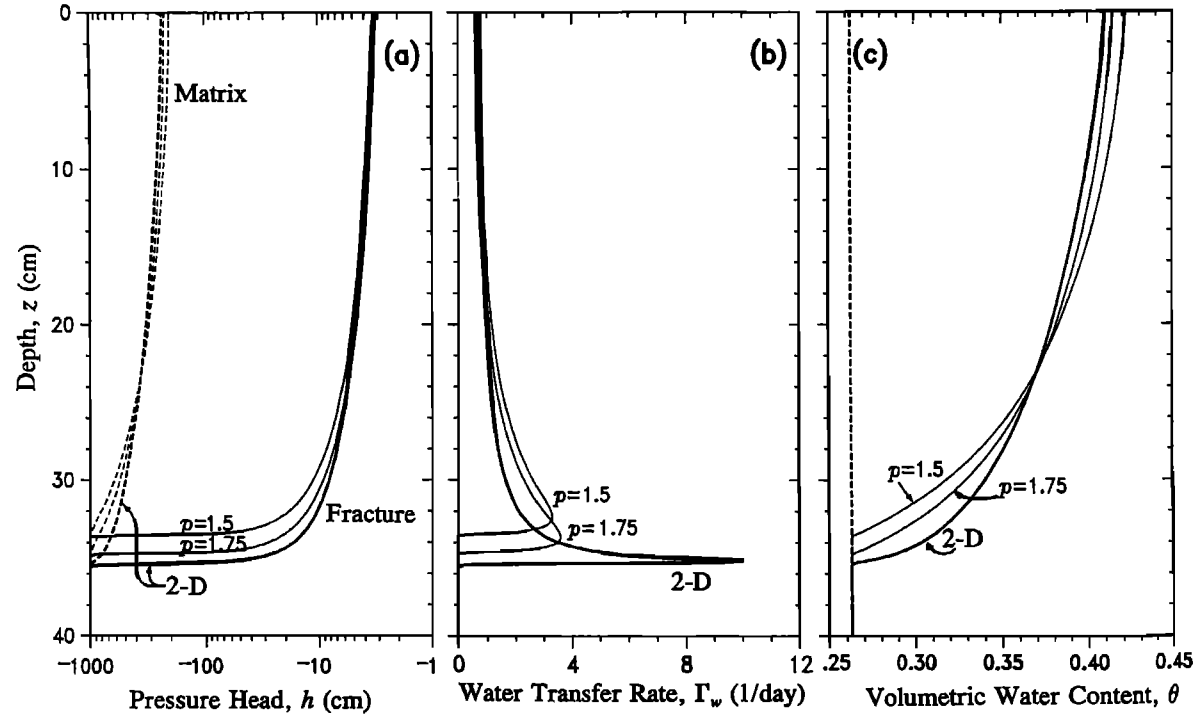

Fig. 8. (*a*) Pressure head h, (*b*) water transfer rate Γ_w, and (*c*) total volumetric water content θ versus depth z at t = 0.08 days as calculated with the one-dimensional dual-porosity (Dual) and two-dimensional (2-D) models. Results are for different p values (first scenario, assuming p = 1.5 with γ_w = 0.04, p = 1.75 with γ_w = 0.002, β = 3, a = 1 cm, and $K_{s,a}$ = 0.01 cm/d).

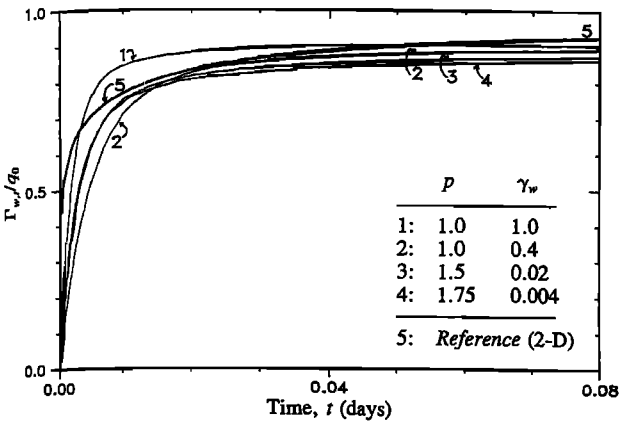

Fig. 9. Plot of the depth-integrated water transfer rate $\Gamma_{w,t}$ as a fraction of the infiltration rate q_0 at the soil surface versus time t as calculated with the dual-porosity and two-dimensional models using different scaling coefficients γ_w and p values (first scenario; $K_{s,a}$ = 0.01 cm/d).

however, the water transfer rates (Figure 7*b*) near the moisture front were still greatly underestimated. As shown in Figure 8, the agreement with the reference calculations could be improved somewhat by using a more nonlinear formulation assuming $p = 1.5$ and $\gamma_w = 0.02$. The match was slightly better when using $p = 1.75$ and $\gamma_w = 0.004$; still, the calculated water transfer rate near the moisture front remained too low.

Figure 9 shows a plot versus time of the depth-integrated water transfer rate, $\Gamma_{w,t} = \int_0^l \Gamma_w \, dz$ (where l is the depth of the profile being considered), as a fraction of the infiltration rate q_0 at the soil surface. The ratio $\Gamma_{w,t}/q_0$ reflects the relative accuracy of the different formulations for Γ_w during the simulation period. The case without scaling (curve 1) resulted in a water transfer/infiltration ratio which soon exceeded that of the reference simulation. The ratio $\Gamma_{w,t}/q_0$ obtained with the dual-porosity model using $p = 1.0$ and $\gamma_w = 0.4$ was initially too low but later, starting at about 0.01 days, seemed to match the reference curve the best. Using more nonlinear expressions (curves 3 and 4 in Figure 9) gave better agreements with the two-dimensional results only until 0.01–0.02 days.

The results in Figures 7, 8, and 9 are best explained by considering the temporal and spatial variations in the water transfer rates. As compared to the reference simulations, the dual-porosity model underestimates water transfer rates at and near the moisture front but later overpredicts the rates at shallower depths (compare Figures 7*b* and 8*b*). Hence the infiltration front calculated with the dual-porosity model using $p = 1.0$ and $\gamma_w = 0.4$ moves initially faster downward as compared to the reference simulation since less water is being transferred into the matrix pore system near the toe of the moisture front. After about 0.02 days, the integrated water transfer rates of the dual-porosity model becomes nearly equal to those of the reference simulation (Figure 9). Because now relatively more water is being removed from the fracture pore system in the upper part of the soil profile (Figure 7*b*), the vertical flow rates in the fractures at larger depths slowly start to decrease.

We also made several comparisons between the one-dimensional dual-porosity model and the two-dimensional model for the second scenario involving both horizontal and vertical water flow in the matrix pore system. The results shown in Figure 10 for the lower transfer rate ($K_{s,a}$ = 0.01 cm/d) were found to be very similar to those in Figure 7 for

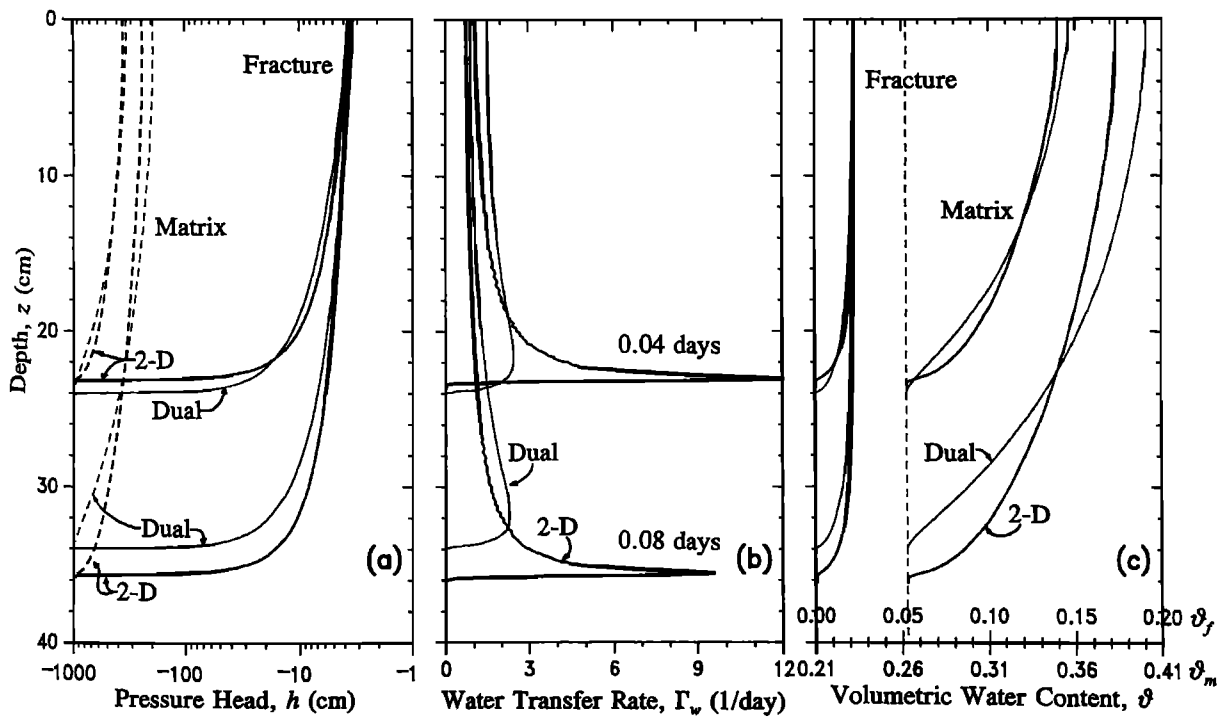

Fig. 10. (*a*) Pressure head h, (*b*) water transfer rate Γ_w, and (*c*) volumetric water content ϑ versus depth z at t = 0.04 and 0.08 days as calculated with the dual-porosity (Dual) model using $p = 1$ and $\gamma_w = 0.4$ and the two-dimensional (2-D) model (second scenario; $K_{s,a}$ = 0.01 cm/d). The water contents $\vartheta_f = w_f\theta_f$ and $\vartheta_m = (1 - w_f)\theta_m$ are in terms of the bulk soil volume; the dotted line in Figure 10*c* indicates the initial water content.

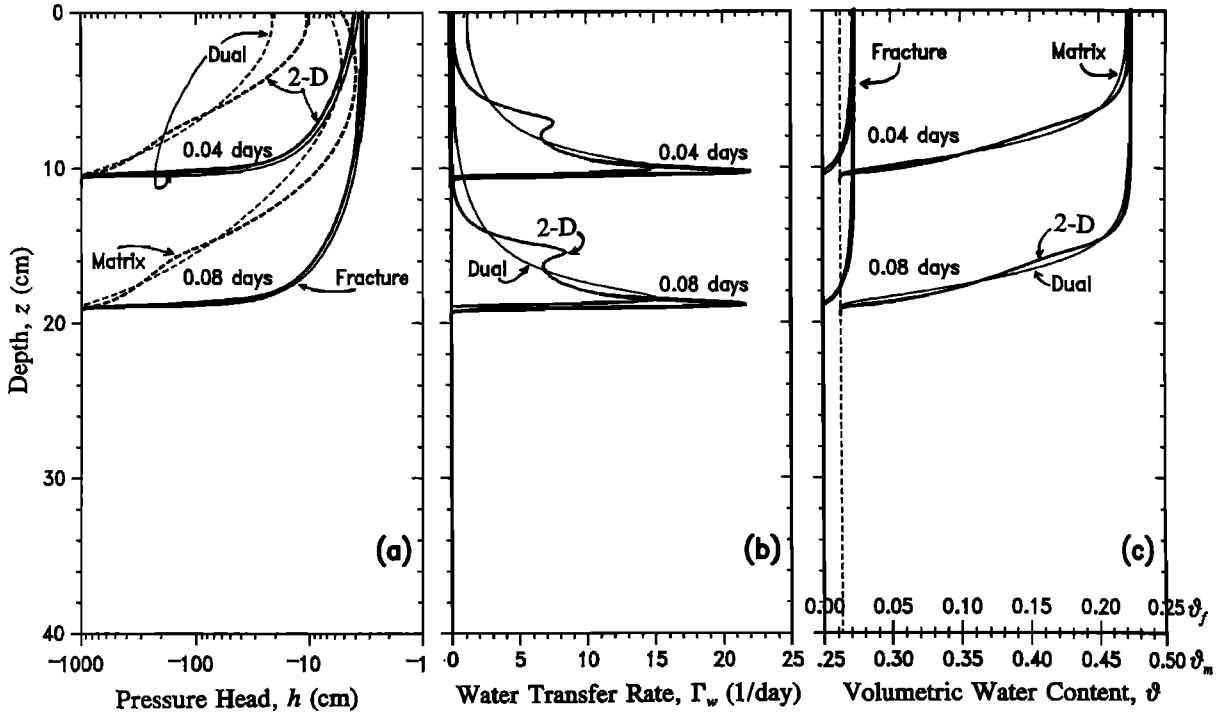

Fig. 11. (*a*) Pressure head h, (*b*) water transfer rate Γ_w, and (*c*) volumetric water content ϑ versus depth z at t = 0.04 and 0.08 days as calculated with the dual-porosity (Dual) model using p = 1 and γ_w = 0.4, and the two-dimensional (2-D) model (second scenario; $K_{s,a}$ = 0.1 cm/d).

scenario one without vertical flow. The similarity is a consequence of the relatively low vertical hydraulic conductivities, and hence flow rates, in the matrix pore system for the prevailing pressure heads. Thus small changes in the already low flow rates did not significantly affect the water transfer rates. We noticed that scenario two (Figure 10) at t = 0.08 days caused the infiltration front to become slightly deeper and the maximum water transfer rate to become somewhat lower as compared to scenario one (Figure 7). The dual-porosity results using p = 1.0 and γ_w = 0.4 matched the pressure head (Figure 10*a*) and water content (Figure 10*c*) profiles of the reference model well in both pore systems at t = 0.04 days; deviations between the two models were slightly larger at t = 0.08 days.

For higher water transfer rates ($K_{s,a}$ = 0.1 cm/d), the agreement between the one- and two-dimensional formulations was generally found to be much closer than those for the lower transfer rates. Results for one set of calculations for the second scenario with p = 1.0 and γ_w = 0.4 are shown in Figure 11. Transfer rates in this case were so large that the pressure heads in the two pore systems approached equilibrium within approximately 10 cm from the infiltration front (see also Figure 6*b*). Notice that the transfer rate profiles calculated with the two-dimensional model (Figure 11*b*) exhibit a relatively small second peak approximately 4 cm above the moisture front. This interesting feature was found only in calculations for the second scenario assuming relatively high water transfer rates. The second peak in Γ_w developed at depths where lateral pressure head nonequilibrium inside the matrix still existed and where vertical flow in the wetted matrix region close to the fracture boundary had accelerated. The presence of two peaks in Γ_w was found to depend strongly on the shape of the hydraulic functions in the particular pressure head range. Notwithstanding the second peak, the average pressure head (Figure 11*a*) and water content (Figure 11*c*) profiles obtained with the two models matched each other very closely in both pore systems.

Finally, we noticed that the more nonlinear formulations caused the scaling coefficient to become increasingly dependent on the pressure head gradient at the fracture/matrix boundary, to the point that for large gradients the dual-porosity scheme became numerically unstable. In particular, for $K_{s,a}$ = 0.1 cm/d, the higher exponent (p = 1.75) gave unacceptable results at early times, while all nonlinear cases yielded poor results also at later times. Considering the results of all calculations carried out in this study, we conclude that a transfer term with p = 1.0 and γ_w = 0.4 performed best.

Discussion and Conclusions

An important characteristic of dual-porosity models is the coupling term Γ_w governing the exchange of water between the fracture and matrix pore systems. This term may be modeled, macroscopically, by means of a first-order rate equation which assumes that water transfer is proportional to the difference between the average pressure heads of two pore systems. Because of its simplicity, Γ_w can simulate the complex three-dimensional local flow process at and across the fracture/matrix interface only in a very approximate manner. Hence, some errors in the dual-porosity model should be expected.

The potential errors involved were studied by comparing dual-porosity model calculations directly with those obtained with equivalent one- and two-dimensional single-

porosity numerical flow models. The test cases involved transient preferential flow in variably saturated structured soil. The two-dimensional model revealed the development of highly nonuniform flow fields inside the matrix pore system along the fracture/matrix interface (see also Figure 6*a*). This was especially true for scenario 2 when relatively large matrix blocks were used. These nonuniform flow fields, of course, cannot be simulated with a one-dimensional dual-porosity model.

This study indicates accurate results for matrix block geometries in the form of parallel rectangular slabs when the dual-porosity model uses a simple arithmetic average of the matrix hydraulic conductivities evaluated at the matrix and fracture pressure heads, together with a single, constant scaling coefficient, γ_w, of 0.4 in equation (3). While improving the results in a few cases, more nonlinear terms caused an increased dependency of the scaling coefficient on the pressure head gradient between the two pore systems.

The relatively simple first-order water transfer term used in this study contains parameters that can be related explicitly to physical properties of the medium, such as the geometry and size of the matrix blocks or soil aggregates, and the hydraulic conductivity K_a of the matrix at the fracture/matrix boundary. Having an explicit dependency of Γ_w on K_a in the flow model is crucial when trying to quantify the potentially very important effects of fracture coatings or other physical and chemical conditions or processes (including weathering) on water flow rates in structured media. *Thoma et al.* [1992] showed that the presence of a mineralized layer or coating at the fracture/matrix interface can significantly reduce the uptake of water into the rock matrix. We showed preferential flow simulation results using a reduction of 0.01 in K_a as compared to K_m (Figure 10); Thoma et al. found even larger reductions.

Still needed is an extension of the transient dual-porosity flow/transport model to other geometries, as well as to systems having a mixture of aggregates of different shapes and sizes, e.g., using methods as suggested by *Rappoldt* [1990]. This problem is currently being investigated. However, and alternatively, one could also treat the dual-porosity model in a more pragmatic manner by considering the geometry coefficient β or better perhaps the entire term $\beta\gamma_w/a^2$ in (3), as an essentially empirical quantity which must be calibrated to observed field data. Overall, however, we believe that the accuracy of the proposed first-order term may be sufficient for most practical applications when considering the large number of uncertainties involved in modeling and measuring preferential flow processes in heterogeneous, structured media. As such, we believe that the dual-porosity model will be helpful for studying field-scale solute transport problems.

Acknowledgments. We thank J. Šimůnek and T. N. Vogel for their help in modifying the SWMII computer model for our simulations.

REFERENCES

Barenblatt, G. I., I. P. Zheltov, and I. N. Kochina, Basic concepts in the theory of seepage of homogeneous liquids in fissured rocks, *J. Appl. Math. Mech.*, *24*(5), 1286–1303, 1960.

Beven, K. J., and R. T. Clarke, On the variation of infiltration into a homogeneous soil matrix containing a population of macropores, *Water Resour. Res.*, *22*, 383–388, 1986.

Bibby, R., Mass transport of solutes in dual-porosity media, *Water Resour. Res.*, *17*, 1075–1081, 1981.

Bolt, G. H., Movement of solutes in soil: Principles of adsorption/exchange chromatography, in Soil Chemistry, B: Physico-Chemical Models, edited by G. H. Bolt, *Dev. Soil Sci. 5B*, 295–348, 1979.

Brusseau, M. L., and P. S. C. Rao, Modeling solute transport in structured soils: A review. *Geoderma*, *46*, 169–192, 1990.

Carslaw, H. S., and J. C. Jaeger, *Conduction of Heat in Solids*, Oxford University Press, New York, 1950.

Chen, C., and R. J. Wagenet, Simulation of water and chemicals in macropore soils, I, Representation of the equivalent macropore influence and its effect on soil-water flow, *J. Hydrol.*, *130*, 105–126, 1992*a*.

Chen, C., and R. J. Wagenet, Simulation of water and chemicals in macropore soils, II, Application of linear filter theory, *J. Hydrol.*, *130*, 127–149, 1992*b*.

Coats, K. H., and B. D. Smith, Dead end pore volume and dispersion in porous media, *Soc. Petrol. Eng. J.*, *4*, 73–84, 1964.

Davidson, M. R., A Green-Ampt model of infiltration in a cracked soil, *Water Resour. Res.*, *20*, 1685–1690, 1984.

Davidson, M. R., Numerical calculation of saturated-unsaturated infiltration in a cracked soil, *Water Resour. Res.*, *21*, 709–714, 1985.

Dudley, A. L., R. R. Peters, J. H. Gauthier, M. L. Wilson, M. S. Tierney, and E. A. Klavetter, Yucca Mountain Project, Total system performance assessment code (TOSPAC), vol. 1, Physical and mathematical bases, *Sandia Rep. Sand85-0002*, Sandia Natl. Lab., Albuquerque, N. M., 1988.

Duguid, J. O., and P. C. Y. Lee, Flow in fractured porous media, *Water Resour. Res.*, *13*, 558–566, 1977.

Dykhuizen, R. C., Transport of solutes through unsaturated fractured media, *Water Res.*, *21*, 1531–1539, 1987.

Dykhuizen, R. C., A new coupling term for dual-porosity models, *Water Resour. Res.*, *26*, 351–356, 1990.

Gaudet, J. P., H. Jégat, G. Vachaud, and P. J. Wierenga, Solute transfer, with exchange between mobile and stagnant water, through unsaturated sand, *Soil Sci. Soc. Am. J.*, *41*, 665–671, 1977.

Gerke, H. H., and M. T. van Genuchten, A dual-porosity model for simulating the preferential movement of water and solutes in structured porous media, *Water Resour. Res.*, *29*, 305–319, 1993.

Gish, T. J., and A. Shirmohammadi (Eds.), *Preferential Flow, Proceedings of the National Symposium, 16–17 December 1991, Chicago, Illinois*, 408 pp., American Society of Agricultural Engineers, St. Joseph, Mich., 1991.

Hoogmoed, W. B., and J. Bouma, A simulation model for predicting infiltration into cracked clay soil, *Soil Sci. Soc. Am. J.*, *44*, 458–461, 1980.

Jarvis, N. J., P.-E. Jonasson, P. E. Dik, and I. Messing, Modelling water and solute transport in macroporous soil. I. Model description and sensitivity analysis, *J. Soil Sci.*, *42*, 59–70, 1991.

Kool, J. B., and M. T. van Genuchten, HYDRUS, One-dimensional variably saturated flow and transport model, including hysteresis and root water uptake, *Res. Rep. 124*, U.S. Salinity Lab., U.S. Dep. of Agric., Agric. Res. Serv., Riverside, Calif., 1991.

Moench, A. F., Double-porosity models for a fissured groundwater reservoir with fracture skin, *Water Resour. Res.*, *20*, 831–846, 1984.

Othmer, H., B. Diekkrüger, and M. Kutilek, Bimodal porosity and unsaturated hydraulic conductivity, *Soil Sci.*, *152*(3), 139–150, 1991.

Parker, J. C., and A. J. Valocchi, Constraints on the validity of equilibrium and first-order kinetic transport models in structured soils, *Water Resour. Res.*, *22*, 399–407, 1986.

Pellett, G. L., Longitudinal dispersion, intraparticle diffusion and liquid-phase mass transfer during flow through multi-particle systems, *Tappi*, *49*, 75–82, 1966.

Peters, R. R., and E. A. Klavetter, A continuum model for water movement in an unsaturated fractured rock mass, *Water Resour. Res.*, *24*, 416–430, 1988.

Raats, P. A. C., Transport in structured porous media, *Proc. Euromech.*, *143*, 221–226, 1981.

Rappoldt, C., The application of diffusion models to an aggregated soil, *Soil Sci.*, *150*, 645–661, 1990.

Rasmuson, A., and I. Neretnieks, Exact solution for diffusion in

particles and longitudinal dispersion in packed beds, *J. Am. Inst. Chem. Eng.*, *26*, 686–690, 1980.

Skopp, J., W. R. Gardner, and E. J. Tyler, Miscible displacement in structured soils: Two region model with small interaction, *Soil Sci. Soc. Am. J.*, *45*, 837–842, 1981.

Sudicky, E. A., The Laplace transform Galerkin technique for efficient time-continuous solution of solute transport in double-porosity media, *Geoderma*, *46*, 209–232, 1990.

Thoma, S. G., D. P. Gallegos, and D. M. Smith, Impact of fracture coatings on fracture/matrix flow interactions in unsaturated, porous media, *Water Resour. Res.*, *28*, 1357–1367, 1992.

Valocchi, A. J., Use of temporal moment analysis to study reactive solute transport in aggregated porous media, *Geoderma*, *46*, 233–247, 1990.

van Genuchten, M. T., A closed-form equation for predicting the hydraulic conductivity of unsaturated soils, *Soil Sci. Soc. Am. J.*, *44*, 892–898, 1980.

van Genuchten, M. T., A general approach for modeling solute transport in structured soils, *Memoires Int. Assoc. Hydrogeol.*, *17*(2), 513–526, 1985.

van Genuchten, M. T., and F. N. Dalton, Models for simulating salt movement in aggregated field soils, *Geoderma*, *38*, 165–183, 1986.

van Genuchten, M. T., and P. J. Wierenga, Mass transfer studies in sorbing porous media, I, Analytical Solutions, *Soil Sci. Soc. Am. J.*, *40*, 473–480, 1976.

van Genuchten, M. T., D. E. Rolston, and P. F. Germann (Eds.), Transport of water and solutes in macropores, *Geoderma*, *46*(1–3), 1–297, 1990.

Vogel, T. N., SWMII—Numerical model of two-dimensional flow in a variably saturated porous medium, *Res. Rep. 87*, Dep. of Hydraul. and Catchment Hydrol., Agric. Univ., Wageningen, Netherlands, 1987.

Wang, J. S. Y., Flow and transport in fractured rocks, *U.S. Natl. Rep. Int. Union Geod. Geophys. 1987–1990*, *Rev. Geophys.*, *29*, suppl., 254–262, 1991.

Warren, J. E., and P. J. Root, The behavior of naturally fractured reservoirs, *Soc. Petrol. Eng. J.*, *3*, 245–255, 1963.

Warrick, A. W., Numerical approximations of Darcian flow through unsaturated soil, *Water Resour. Res.*, *27*, 1215–1222, 1991.

Wilson, M. L., and A. L. Dudley, Radionuclide transport in an unsaturated, fractured medium, in *Flow and Transport Through Unsaturated Fractured Rock, Geophys. Monogr. Ser.*, vol. 42, edited by D. D. Evans and T. J. Nicholson, pp. 23–29, AGU, Washington, D. C., 1987.

Workman, S. R., and R. W. Skaggs, PREFLO: A water management model capable of simulating preferential flow, *Trans. ASAE*, *33*(6), 1939–1948, 1990.

Zimmerman, R. W., and G. S. Bodvarsson, Integral method solution for diffusion into a spherical block, *J. Hydrol.*, *111*, 213–224, 1989*a*.

Zimmerman, R. W., and G. S. Bodvarsson, An approximate solution for one-dimensional absorption in unsaturated porous media. *Water Resour. Res.*, *25*, 1422–1428, 1989*b*.

Zimmerman, R. W., G. S. Bodvarsson, and E. M. Kwicklis. Adsorption of water into porous blocks of various shapes and sizes, *Water Resour. Res.*, *26*, 2797–2806, 1990.

H. H. Gerke, Destedter Haupstrasse 1, D-3302 Gremlingen, Germany.

M. T. van Genuchten, U.S. Salinity Laboratory, Agricultural Research Service, USDA, 4500 Glenwood Drive, Riverside, CA 92501.

(Received April 17, 1992;
revised September 24, 1992;
accepted October 14, 1992.)